RESEARCH PAPER

Analysis of a folded reflect-array antenna using particle swarm optimization

SABINE DIETER, CHRISTOPH FISCHER AND WOLFGANG MENZEL

In this paper, a method for design and optimization of folded reflect-array antennas is proposed based on particleswarm optimization (PSO). In addition to such a powerful optimization algorithm, two further requirements have to be fulfilled. The first one is a good and fast algorithm for the exact prognosis of the far-field radiation diagram, resulting from a specific element configuration on the reflector. Additionally, a good choice of the fitness function for the evaluation of the resulting radiation diagrams is necessary. In both, reflect-array-related aspects such as phase truncation, reflection losses, and cell discontinuities have to be considered. Antenna optimization based on this technique is presented in this paper at the example of two 77 GHz folded reflect-array antennas. The efficiency of this approach is demonstrated with these examples, and the results are verified by measurement, showing an excellent agreement with the specifications of the diagram masks. The implemented tool, including a realistic antenna diagram preview, allows the investigation of the design parameters' influence on the antenna performance, such as illumination amplitude, high substrate losses, and phase truncation.

I. INTRODUCTION

Planar reflect-array antennas [1] show the advantages of compact size, low weight, reduced cost, and easy fabrication. The principle of folded reflect-array antennas [2] is illustrated in Fig. 1.

The input wave from the feed is reflected at the polarization grid. Then, a second reflection occurs, this time on the lower reflector, which is designed as an array of reflector elements, e.g. metallized rectangular patches on a backside-metallized substrate. Due to a polarization twist on the array, the wave then passes the polarization grid. Additionally, the reflection elements act as phase shifters, which compensate for free-space phase delays and add specific phase angles. In this way, a multitude of far-field diagrams can be synthesized.

Optimization methods for such folded reflect-array antennas have been investigated in the past, e.g. with Newton's method [3]. The principle of the presented optimization process for the reflect-array antenna is shown in Fig. 2. In the first step, the antenna diagram is calculated for a set of input parameters, which will be discussed in Section II. The resulting output diagram F should be very accurate, as the whole further proceedings will depend on these results. The difference between the desired antenna diagram (specification mask) and the calculated intermediate results is evaluated by the fitness function, see Section III. If the achieved diagram fulfills the antenna requirements given by the mask, the actual

University of Ulm, Institute of Microwave Techniques, 89069 Ulm, Germany.
Phone: +49 731 5026377.
Corresponding author:
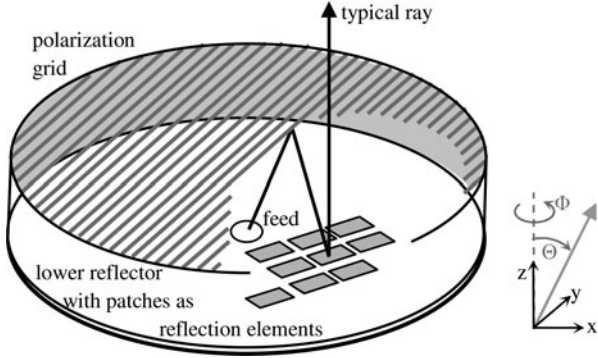S. Dieter
Email: sabine.dieter@uni-ulm.de

configuration could be chosen to be the final design, this would terminate the process. Otherwise, in the next iteration, the diagram calculation is restarted with a new set of input parameters. The criteria for the chosen new parameters are based on the respective optimization algorithms and also depend on already achieved results from previous iterations. The features of the used algorithms are explained in Section IV.

II. COMPUTATION OF THE ANTENNA DIAGRAM

Besides the chosen optimization algorithm, the realistic prediction of an antenna diagram, resulting from a given configuration of the reflector at a certain frequency point, is an important requirement for the whole process. For this purpose, a mathematical tool has been developed for the diagram extraction, which makes use of the following steps:

– The free-space phase delay of the incident electrical field on the lower reflector is calculated by quasi-optical ray tracing.
– The amplitude of the incident electrical field on the lower reflector is determined. Therefore, the radiation pattern of the feed has been incorporated in the quasi-optical model [4].
– The complex reflection coefficient for each patch on the reflector surface is computed by use of a frequency-selective-surface (FSS) simulation tool [5]. Dependent on the used FSS unit cell, not all phase angles can be realized. At a frequency of 77 GHz, the complex reflection coefficient is computed dependent on the dimensions of rectangular structures as they are shown in Fig. 1.

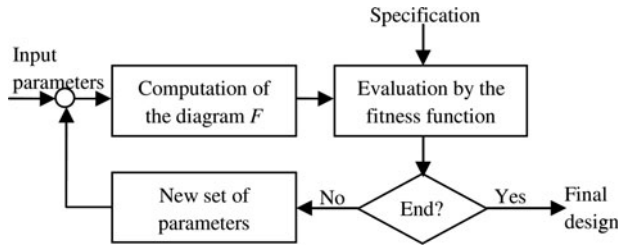**Fig. 1.** Principle of a folded reflect-array antenna.

Fig. 2. Optimization process of the antenna.

According to these points, both the phase angles as well as the amplitude distribution are considered where the amplitude depends on the feed illumination and the reflection amplitude of each reflect-array cell. Tests have shown that especially the amplitude of the illumination has an important influence and must not be neglected in order to obtain a realistic estimation of the resulting far-field diagram. To take into account the effect of the element diagram of each reflector, a correction factor $\cos \Theta$ is multiplied with the resulting group diagram $F_{Group}(\Theta, \Phi)$, which is also called array factor of a group antenna:

$$F(\Theta, \Phi) = \cos \Theta F_{Group}(\Theta, \Phi) \tag{1}$$

This factor $\cos \Theta$ is only a simplified assumption of the element diagram of a single patch on the reflector. However, this approximation is sufficient, as can be seen in the comparison between the simulated and measured antenna diagrams (Fig. 3) of a folded reflect-array antenna with design criteria also used in Section V.
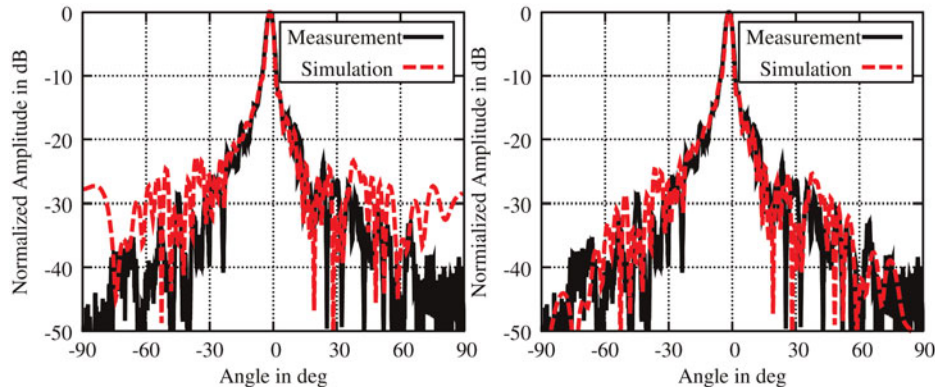
III. FITNESS FUNCTION

The definition of the fitness function is an important factor for the quality of the final optimization result. Here, the fitness function evaluates the far-field diagram resulting from a given configuration of the reflector structure, as shown in Fig. 2. The output parameter is a scalar value, which stands for the deviation between the achieved diagram and an ideal reference mask. An example of a pencil beam far-field diagram and a corresponding mask is given in Fig. 4. The fitness function evaluates the gain of the antenna, its 3 dB beam width and the side-lobe suppression as well. Here, the evaluation is done by upper mask limits (e.g. -30 dB in the marked region of the side lobes in Fig. 4.) and lower mask limits – for the pencil beam diagram in Fig. 4, only a lower limit in the region of the main beam is reasonable. The angular position of this mask determines the desired beam width.

Besides the far-field diagram, in this work, the fitness function includes an additional criterion for evaluation of the reflector configuration. On the one hand, the design of a reflect-array has the freedom of an overall absolute phase angle offset. On the other hand, the phase angle range of the elements is limited, resulting in phase angle steps of $360°$ and large changes of adjacent patch geometries. The choice of the overall phase angle offset allows using a reflector
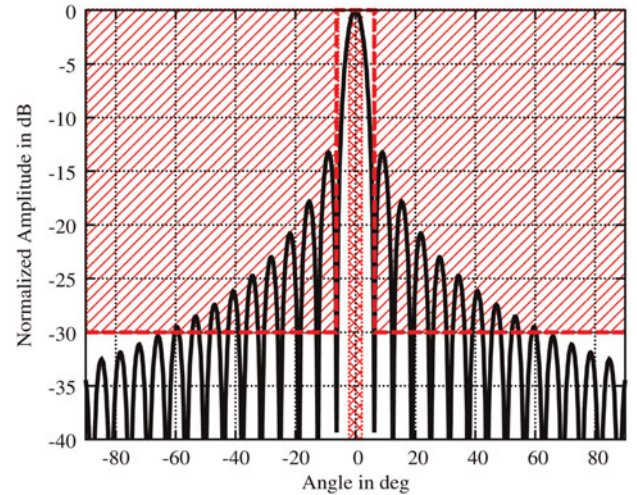

Fig. 4. Example of the antenna mask for a pencil beam diagram.

Fig. 3. Comparison between measured and simulated results of a folded reflect-array antenna without (left) and with diagram correction by the element factor (right).

configuration with small changes of geometries in the strong illuminated regions of the reflect-array. This behavior is also included in the fitness function, allowing optimal reduction of such large elements' variations. Thus, by calculating geometrical differences of adjacent patch elements, the continuity of the geometrical patch dimensions on the reflector surface is taken into account. In order to evaluate the geometrical continuity for a current reflector design, the difference of adjacent reflector elements is summed up in x- and y-dimension on the reflector and weighted with a constant factor.

IV.   OPTIMIZATION PROCESS

Particle swarm optimization (PSO) was introduced in [6, 7] as a powerful optimization method, using a swarm of birds as a model for the algorithm. Based on this example given by nature, swarms of particles identifying possible solutions of a problem, move through the solution space and use personal and group memory in order to find an optimum solution. There exist several publications based on this algorithm presented in [6], only a few important for this work are listed here [7–9]. As this method is applicable in all fields of science, it is also suitable for optimization problems in the microwave area, e.g. in [8].

The detailed application for this algorithm is explained in [10] and is combined with a very effective method introduced in [11] in order to decrease the number of parameters that have to be optimized. Instead of optimizing the phase of each reflector element, only the weights of the basis functions, describing the phase distribution on the reflector, are optimized. This rigorously reduces the number of parameters and therefore enforces rapid convergence. This principle was adapted within this approach and could reduce the number of parameters within the optimization process from $N = 2000$ to a number of $N < 8$.

In the overall process, as shown in Fig. 2, the choice of new parameters assumes a continuous phase angle distribution, but the computation of the diagram still uses single-patch properties, such as phase truncation and the magnitude of the reflection coefficient. The overall process has the advantage of fast optimization, combined with a better performance due to the consideration of the single-patch behaviour in the antenna diagram computation and the consideration of the cell geometries.

V.   MEASUREMENT RESULTS

The general specifications of the optimized and fabricated folded reflect-array antennas are listed in Table 1. First, we present an antenna design based on the parameters in Table 1 and cosec^2 characteristics. The diagram mask can be seen in Fig. 5. The used substrate is RT-Duroid 5880 from Rogers with a permittivity $\varepsilon_r = 2.2$ and a thickness of 0.127 mm.

Figure 5 shows both the simulation and measurement result of the cosec^2 antenna. The optimization routine results in a good match between specification and measurement. Even better results have been achieved for the design of an offset-beam antenna with main beam at $\Theta = -25°$, see Fig. 6. The chosen substrate was RO4003C from Rogers with the permittivity $\varepsilon_r = 3.38$ and a thickness of 0.51 mm. The results show a very good optimization performance regarding reduced side-lobe level and small beam width of the main beam. Figure 6 also shows a good matching between theory and measurement results. The two curves are almost identical. A slightly increased side-lobe level in

Table 1. Specifications of the fabricated folded reflect-array antennas.

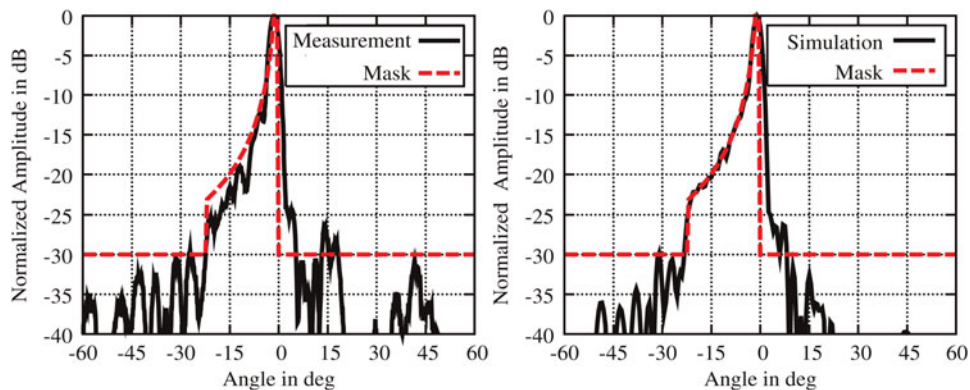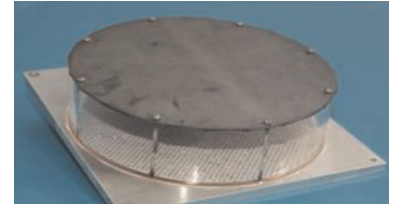|	
Frequency	77 GHz
Reflection elements	ca. 2000
Antenna diameter	123 mm
Antenna height	30 mm
Unit cell size on the array	2.14 mm × 2.14 mm
Antenna diagrams	cosec^2 and offset-beam

Fig. 5. Comparison between measurement and simulation for the optimized cosec^2 antenna.
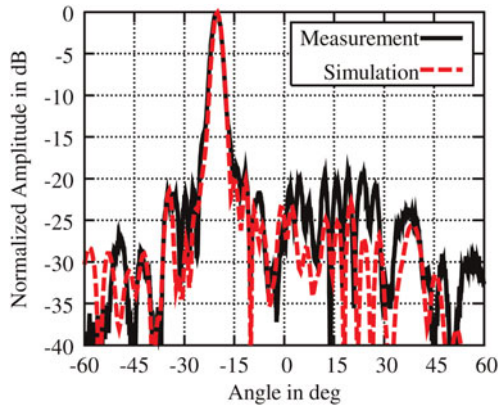
Fig. 6. Comparison between simulated diagram after optimization and corresponding measured diagram for the offset-beam antenna at 77 GHz.

the measurements are caused by non-ideal effects, some of those are phase errors and depolarization effects due to fabrication tolerances and due to edge effects, surface waves, and specular radiation effects on the reflector.

Compared to other optimization methods used for design of folded reflect-array antennas [3], very good results could be achieved for that antenna type with the presented method. Because of the different requirements of the respective antenna designs the optimization results cannot be compared directly.

VI. INVESTIGATIONS OF DESIGN PARAMETERS

The precise diagram computation feature included in the described tool enables the analysis of the impact of design restrictions on the resulting antenna diagram, such as phase truncation, amplitude effects, and the usage of substrates with higher losses.

A) Phase truncation

Single-layer unit cells usually cover a phase angle range of less than 360°. One degree of freedom concerning the reflector configuration is an overall phase angle offset. The impact of this offset is investigated with the developed antenna design tool (Fig. 7).

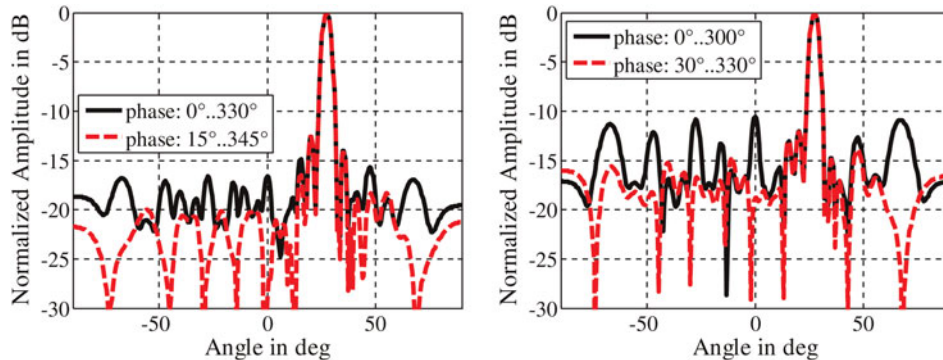The compared antenna diagrams, both optimized for an offset beam at 30°, are designed on the basis of unit cells, covering all possible phase angles. After that a phase truncation was introduced affecting the range from 330 to 360° (Fig. 7 left) and 300 to 360° (Fig. 7 right). For each configuration, the respective antenna patterns are shown without angular offset and using an offset that reduces the degradation of the pattern. As expected, it turns out that a phase angle error symmetrically distributed over the reflector results in a lower side lobe level. Apart from that, it is important to avoid large phase error in regions that essentially contribute to the antenna pattern, e.g. the strongly illuminated center region of the antenna.

B) Influence of amplitude effects

Besides the phase errors also the influence of the amplitude of the incident and reflected field was investigated. The results are show in Fig. 8, which compares the far-field diagram for one reflector configuration with three methods of diagram computation including phase-only process, one method with illuminating amplitude but no reflection amplitude and the most accurate version considering both amplitude effects. Here, the reflector configuration is the same for all three diagram curves. The difference is that certain effects concerning the amplitude distribution on the reflector are neglected during pattern computation. For common radio frequency (RF) substrates with their low reflection losses, the effect on the elementary cell's reflection amplitude is small. But the illumination of the reflector may not be neglected, as one can see in the differing computed diagrams with phase-only or constant amplitude conditions (Fig. 8).
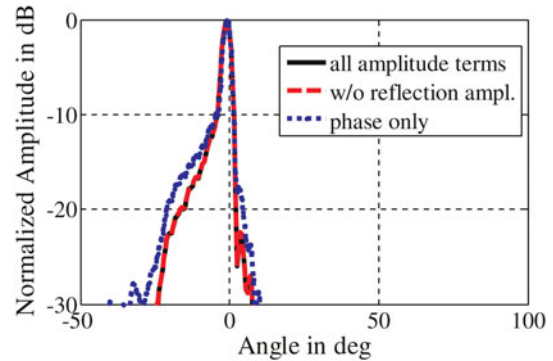

Fig. 8. Consideration of different amplitude effects in diagram computation for a certain reflector configuration.
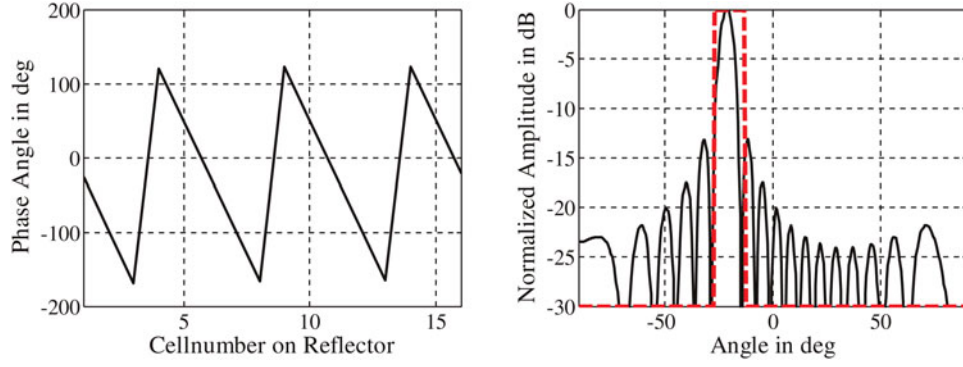

Fig. 7. Influence of a phase offset in the reflector design for unit cells with total phase angle range of 330° (left) and 300° (right).

Fig. 9. Ideal phase angle on the reflector (left) and corresponding offset beam diagram with phase-only optimization (right).
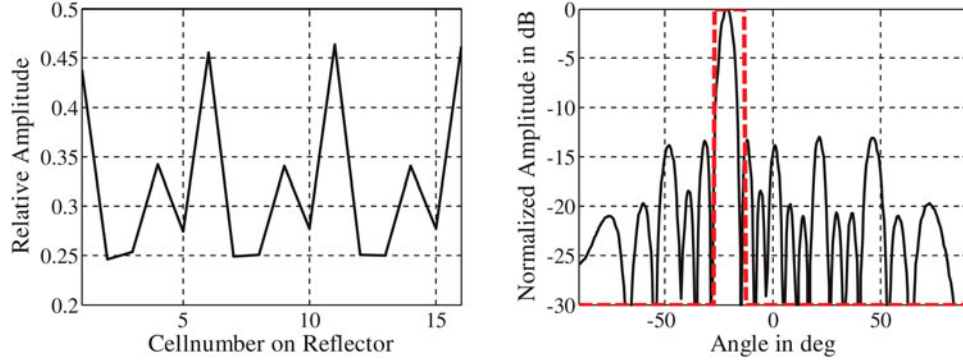

Fig. 10. Relative amplitude on the reflector using a substrate with high losses (left) and corresponding simulated antenna diagram with high side lobes (right).

C) Substrates with high losses

In the following, another aspect related to the reflection coefficient should be investigated on a fictive, simplified reflect-array antenna in theory. There is a uniform illumination assumed, by a point source in the antenna axis, as the illumination aspects have already been investigated in the previous section. Due to the rotational symmetry only the center row should be considered.

In Fig. 8 one can see, that the magnitude of the reflection coefficient of low-loss substrates can be assumed as $\Gamma = 1$, as only a few elements on the whole reflector operate directly at the resonant length with maximum losses. Assuming lossy dielectrics with a loss tangent in the order of 0.02, we can see another effect on the antenna diagram. For this investigation, a simple centrally fed reflect-array antenna is assumed, which is not folded and consists of 16×16 reflection elements. These fictive unit cells cover the whole phase angle range of $360°$. The expected linear phase angle progression in the center row of the reflector is shown in Fig. 9 (left). The periodicity of the unit cells is chosen to 0.55λ. For the computation of the diagram a constant amplitude distribution is assumed which leads to a side-lobe level of -13 dB (Fig. 9 right).

Consideration of the high losses of the substrate leads to quasi-periodical amplitude drops, whenever a patch is close to resonance, as it is shown in Fig. 10 (left). In the respective antenna diagram, Fig. 10 (right), one can see high side-lobes at regular angular distances θ. They can be calculated by

$$\theta = \arcsin\left[\frac{\lambda}{d}\left(\frac{2k+1}{2} + \frac{\Delta\varphi}{2\pi}\right)\right] \qquad (2)$$

whereas $k \in Z$ is the side-lobe order, d the periodic distance of cell points with amplitude drop, and $\Delta\varphi$ is the linear-phase-angle progression between adjacent cell points. From Fig. 10 (left) a periodicity of five cells can be obtained. Applied to (2), the analytically expected and the simulated side-lobe positions are matching. The quasi-periodic amplitude pattern on the reflector acts like a configuration with an equivalent element distance of 2.75λ on the array. Hence, the side lobes can be interpreted as the grating lobes of an under-sampled array.

VII. CONCLUSION

In this paper, the design and optimization of two folded reflect-array antennas for 77 GHz was presented using PSO. It has been shown that by use of a powerful optimization method, an accurate extraction of the antenna diagram from the reflector configuration, and a reasonable choice of the fitness function, convincing optimization results can be achieved. Besides optimizing maximum power in the direction of the main beam, the shape of the antenna diagram can be specified, including the side-lobe level or even more detailed profiles, like e.g. a cosec² characteristic. The functionality of the optimization process is verified by two antenna designs and measurement results for 77 GHz, i.e. one offset-beam antenna and one antenna with a cosec² pattern. The influence of design parameters on the antenna performance, including illumination amplitude, high substrate losses, and phase truncation, were investigated using the developed tool, including the antenna diagram preview.

ACKNOWLEDGEMENTS

REFERENCES

[1] Pozar, D.M.; Targonski, S.D.; Pokuls, R.: A shaped-beam microstrip patch reflectarray. IEEE Trans. Antennas Propag., **47** (1999), 1167–1173.

[2] Menzel, W.; Pilz, D.; Al-Tikriti, M.: Millimeter-wave folded reflector antennas with high gain, low loss, and low profile. IEEE Antennas Propag. Mag., **44** (2002), 24–29.

[3] Zeitler, A.; Lanteri, J.; Pichot, C.; Miglaccio, C.; Feil, P.; Menzel, W.: Folded reflectarrays with shaped beam pattern for foreign object debris detection on runways. IEEE Trans. Antennas Propag, **58** (9) (2010), 3065–3068.

[4] Feil, P.; Mayer, W.; Menzel, W.: A 77 GHz eight-channel shaped beam planar reflector antenna, in 3rd European Conf. on Antennas and Propagation (EuCAP), March 2009, pp. 1320–1323.

[5] ANSYS: Ansoft Designer 5.0.2., ANSYS Inc., Canonsburg, PA, USA, 2010.

[6] Kennedy, J.; Eberhart, R.: Particle swarm optimization, in IEEE Int. Conf. on Neuronal Networks, December 1995, vol. 4, pp. 1942–1948.

[7] Clerc, M.; Kennedy, J.: The particle swarm – explosion, stability, and convergence in a multidimensional complex space. IEEE Trans. Evol. Comput. **6** (2002), 58–73.

[8] Robinson, J.; Rahmat-Samii, Y.: Particle swarm optimization in electromagnetics. IEEE Trans. Antennas Propaga., **52** (2004), 397–407.

[9] Xu, S.; Rahmat-Samii, Y.: Boundary conditions in particle swarm optimization revisited. IEEE Trans. Antennas Propag., **55** (2007), 760–756.

[10] Dieter, S.; Fischer, C.; Menzel, W.: Design of a folded reflectarray antenna using particle swarm optimization. in 40th European Microwave Conf., September 2010, pp. 731–734.

[11] Gatti, R.V.; Maraccioli, L.; Sorrentino, R.: A novel phase-only method for shaped beam synthesis and adaptive nulling, in 33rd European Microwave Conf., October 2003, pp. 739–742.

Sabine Dieter received the Dipl.-Ing. degree from the University of Ulm, Germany in 2007. Since 2007 she is with the Institute of Microwave Techniques, University of Ulm as a research assistant. Her current areas of interest are antenna design, optimization, and characterization.

Christoph Fischer received his Dipl.-Ing. degree from the University of Ulm, Germany in 2010. Since 2010 he is with the Daimler AG Ulm as a research assistant. His current areas of interest are beam forming methods and signal processing for RADAR applications.

Wolfgang Menzel received his Dipl.-Ing. degree at the Technical University of Aachen, Germany, in 1974, and the Dr.-Ing. degree from the University of Duisburg, Germany, in 1977. From 1979 to 1989, he worked in the mm-wave department of AEG (now EADS) in Ulm, Germany, as head of the laboratory for integrated mm-wave circuits, and later as head of the mm-wave department. In 1989, he received a full professorship at the University of Ulm. His current areas of interest are multi-layer planar circuits, waveguide filters and components, antennas, mm-wave and microwave interconnects and packaging, and mm-wave application and system aspects. Dr. Menzel is a fellow of the IEEE.